

Cocaine Congeners as PET Imaging Probes for Dopamine Terminals

Anna-Liisa Brownell, David R. Elmaleh, Peter C. Meltzer, Timothy M. Shoup, Gordon L. Brownell, Alan J. Fischman and Bertha K. Madras

Department of Radiology, Massachusetts General Hospital, Boston, Massachusetts; Organix Inc., Woburn, Massachusetts; and Harvard Medical School and New England Regional Primate Research Center, Southborough, Massachusetts

The PET imaging properties of three phenyltropane drugs with differing affinities and selectivities for the dopamine over serotonin transporter, were compared. **Methods:** Carbon-11-CFT (WIN 35,428, 2 β -carbomethoxy-3 β -(4-fluorophenyl)tropane), ^{11}C -CCT (RTI-131, 2 β -carbomethoxy-3 β -(4-monochlorophenyl)tropane), and ^{11}C -CDCT (dichloropane, 2 β -carbomethoxy-3 β -(3,4-dichlorophenyl)tropane) were evaluated as imaging probes for dopamine neurons in five normal and in two MPTP-treated cynomolgus monkeys (*macaca fascicularis*) using a high-resolution PET imaging system (PCR-I). **Results:** For ^{11}C -CFT, the specific binding ratio (as defined by the ratio of radioactivity levels in striatum versus cerebellum) was 4.2 ± 0.8 in caudate and 4.9 ± 1.2 in putamen at 60 min and 4.9 ± 1.2 and 5.5 ± 1.1 at 90 min in control animals. In MPTP-treated monkeys the corresponding ratios were 1.4 ± 0.1 in caudate and 1.5 ± 0.1 in putamen at 60 min and 1.3 ± 0.1 in caudate and 1.4 ± 0.3 in putamen at 90 min. For the monochloro analog of CFT, ^{11}C -CCT, the ratios in control caudate and putamen were 2.7 ± 0.4 and 3.4 ± 0.3 , respectively, at 60 min and 3.7 ± 0.5 and 4.4 ± 0.6 , respectively, at 90 min. In MPTP-treated animals, corresponding ratios were 1.4 ± 0.4 and 1.5 ± 0.3 at 60 min and 1.4 ± 0.4 and 1.6 ± 0.4 at 90 min. The dichloro analog of CFT, CDCT, which has the highest affinity for the dopamine transporter, generated the lowest ratios in control brains, 2.3 ± 0.4 in caudate and 2.4 ± 0.5 in putamen at 60 min. In one MPTP-treated monkey, the corresponding ratios were 1.6 ± 0.4 and 1.8 ± 0.3 . In comparison with ^{11}C -CFT, both ^{11}C -CCT and ^{11}C -CDCT were less selective and had high uptake in the thalamus. **Conclusion:** The present results clearly indicate that ^{11}C -CFT is a useful ligand for monitoring dopamine neuronal degeneration.

Key Words: CFT (WIN 35,428); CCT (RTI-131); CDCT (dichloropane); positron emission tomography; Parkinson's disease

J Nucl Med 1996; 37:1186-1192

Parkinson's disease is a neurological disorder which is characterized by the degeneration of dopamine neurons in substantia nigra and depletion of dopamine in striatal terminal fields of these neurons (1). A primary neurochemical consequence of Parkinson's disease is a marked decrease in the concentration of dopamine in the striatum (2). The original observation led to experiments aimed at developing animal models for Parkinson's disease using surgical techniques or neurotoxins selective for dopamine neurons (3). Since cases of human Parkinsonism were discovered after intravenous self-administration of a meperidine analogue, 1-methyl-4-phenyl-1,2,5,6 tetrahydropyridine (MPTP) (4), primate models of Parkinsonism have been developed using different MPTP administration protocols (5-7).

Received March 20, 1995; revision accepted Oct. 8, 1995.

For correspondence or reprints contact: Anna-Liisa Brownell, PhD, Physics Research Laboratory, Department of Radiology, Massachusetts General Hospital, Edwards Building, 5th Floor, Boston, MA 02114.

Several brain imaging agents targeted to the dopamine neurons and associated nerve terminals have been developed to image Parkinson's disease. These positron emission tomographic agents are aimed at monitoring dopamine neurons (8-26). The most commonly used ligand is ^{18}F -fluoro-L-dopa, an analog of the naturally occurring compound, L-DOPA (8-10). However, this compound is metabolizable and striatal accumulation of radioactivity is a reflection, in part, of the activity of an amino acid transporter and of metabolism to ^{18}F -fluoro-dopamine and other ^{18}F -labeled metabolites. Other ligands have been developed, particularly those targeted to the dopamine transporter including ^{11}C -S-nomifensine (11,12), ^{18}F -GBR 13119 (13-15) and ^{11}C -cocaine (16-17). However, nonselective binding of these ligands to sites other than the dopamine transporter has been a major limiting factor for use of these compounds for in vivo imaging.

In search of in vivo probes with high affinity and selectivity for dopamine transporter/neurons, Madras et al. proposed (18-23) the use of phenyltropane analogs of cocaine based on promising data obtained with ^3H -2 β -carbomethoxy-3 β -(4-fluorophenyl) tropane (CFT or WIN 35,428) (18-20). In particular, studies conducted with ^3H -CFT in postmortem human Parkinson's diseased caudate and putamen showed that the depletion of the transporter on dopamine neurons corresponded to the reported loss of dopamine (21).

Tritiated-CFT binding sites in primate striatum displayed a pharmacological specificity consistent with that of the dopamine transporter (18,19) and distributed primarily to brain dopamine systems (20-22). Although selective for the dopamine transporter, the affinity of CFT for the transporter is relatively moderate, 11.0 ± 1.0 nM (18,20,24,25). Mono or dichloro substitution of the fluoro group on the phenyltropane ring yields compounds with approximately 10-fold higher affinity for the dopamine transporter than CFT (WIN 35,428) but with reduced selectivity for the dopamine transporter (24). In this study, the imaging characteristics of ^{11}C -CFT and the higher affinity chloro analogs of CFT, ^{11}C -CCT or RTI-131 (2 β -carbomethoxy-3 β -(4-monochlorophenyl)tropane and ^{11}C -CDCT or dichloropane (2 β -carbomethoxy-3 β -(3,4-dichlorophenyl)tropane) are described and compared in control and in MPTP-treated monkeys.

MATERIALS AND MEASUREMENTS

MPTP Model of Parkinson's Disease

To induce symptomatic parkinsonism, adult (>3.3 kg) male and female cynomolgus monkeys (*macaca fascicularis*) were anaesthetized (15 mg/kg ketamine) and three sequential doses of MPTP (dose 0.7 mg/kg) were administered into the femoral vein within 10 days (6). The primates developed Parkinsonian symptoms shortly after the last injection of MPTP and symptoms persisted as long as

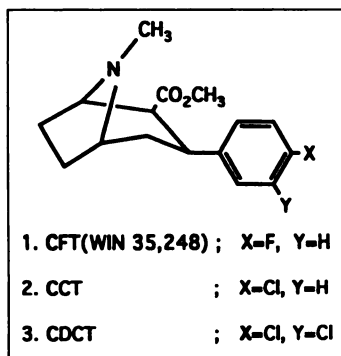


FIGURE 1. Schematic structure of CFT (WIN 35,248, 2 β -carbomethoxy-3 β -(4-fluorophenyl)tropane), CCT (RTI-131,2 β -carbomethoxy-3 β -(4-monochlorophenyl)tropane) and CDCT (dichloropane, 2 β -carbomethoxy-3 β -(3,4-dichlorophenyl)tropane).

for three months, until euthanasia. Animals were maintained with daily intramuscular injections (0.1–0.5 mg/kg) of quinlorane, a D₂ dopamine receptor agonist. Animals used in this study were maintained according to the guidelines of the Committee on Animals of the Harvard Medical School and Massachusetts General Hospital and of the "Guide for Care and Use of Laboratory Animals" of the Institute of Laboratory Animal Resources, National Research Council, Department of Health, Education and Welfare, Publication No. (NIH)85-23, revised 1985.

Radiopharmaceutical Production Carbon-11-CFT, CCT and CDCT

Carbon-11-CFT, ¹¹C-CCT, and ¹¹C-CDCT (Fig. 1) were prepared by direct ¹¹C-methyl iodide methylation of their nor N-demethylated precursors. The nor precursors were synthesized by Organix, Inc. ¹¹C-methyl iodide was produced in an automated system following proton bombardment of N₂ containing 0.5% O₂ to yield ¹¹CO₂. The ¹¹CO₂ was trapped in 0.4 ml of LAH (0.25 M) in THF and dried under a stream of N₂ gas by heating at 120°C. The AlLiO-¹¹CH₃ was treated with 0.8 ml of a 57%-solution of hydroiodic acid. The resulting ¹¹C methyl iodide was then transferred as a gas using N₂ as carrier to a reaction vial containing 400 μ g of N-demethylated precursor (norCFT, norCCT or norCDCT) in 0.3 ml of DMSO and the mixture was heated at 110°C for 5 min. HPLC purification of ¹¹C-CFT (or ¹¹C-CCT or ¹¹C-CDCT) was performed with a Waters C₁₈ reverse-phase column (1 \times 10 cm) using a solvent system of 60% methanol and 40% pH 7.3 buffer (2.75 g KH₂PO₄, 2 ml TEA in 1000 ml water) and flow rate of 2 ml/min. Retention times were 6.5, 7.7 and 9.0 min for ¹¹C-CFT, ¹¹C-CCT and ¹¹C-CDCT, respectively. Radiochemical yield was 15–20% and radiochemical purity >98%. After solvent evaporation, the residue was dissolved in 6-ml saline and the solution was filtered through a 0.22- μ m Millipore filter. The specific activity of the final product was between 600–1000 Ci/mmol. The preparation time of the labeled compound was 23 min.

PET Studies

Imaging System. PET was performed using a high-resolution PET scanning system equipped with one ring of 360 BGO detectors and a computer-controlled imaging table (27). The resolution of PCR-I for a point source at the center of the imaging field is 4.5 mm and the sensitivity is 46,000 counts per sec for a source 20 cm in diameter with a concentration of 1 μ Ci/ml, when the images are reconstructed using Hanning weighted convolution backprojection with cutoff value of 1.0 (28). The overall efficiency is 64% of the theoretical maximum for a plane thickness corresponding to the 2-cm high detectors. A plane thickness of 5 mm, to be used in this study, is obtained by limiting the effective height of the detectors with cylindrical collimators. The coincidence resolving time of PCR-I is 6 nsec (FWHM).

Study Protocol. PET studies were performed with the three different ligands in normal and MPTP-treated cynomolgus monkeys (weight 3.3–4.6 kg). Carbon-11-CFT was used in five control

animals and in five studies with two MPTP-treated monkeys. ¹¹C-CCT was used in two studies in control animals and in one study in an MPTP-treated primate. All MPTP-treated animals had control studies before MPTP treatment. Carbon-11-CDCT was used in one primate before and after MPTP treatment.

For PET imaging, the animals were anaesthetized with ketamine/xylazine (15/1.5 mg/kg, intramuscular, initial dose) and anaesthesia was maintained with half doses hourly as needed. Catheters were placed into the femoral artery and vein for collection of blood samples and injection of labeled ligand. The animal was placed ventrally on imaging table. The head was secured in a customized acrylic head holder equipped with ear and eye bars specially designed to ensure reproducible stereotactic head positioning from study to study. Dynamic imaging data were collected at seven different coronal planes: 30, 25, 20, 15 and 10 mm anterior from the origin, 5 mm and 10 mm posterior from the origin. After injection 1.5 \pm 0.3 nmole/kg of radiolabeled ¹¹C-CFT, or ¹¹C-CCT or ¹¹C-CDCT (3.8–7.9 mCi, specific activity 600–1000 mCi/ μ mole) into the femoral vein, imaging data were collected stepwise at each level using an initial collection time of 15 sec. The collection time was increased up to 60 sec and the total imaging time was 90 min. Calibration of the positron tomograph was performed prior to each study using a cylindrical plastic phantom (diameter 6 cm) containing a solution of ¹⁸F. Six arterial blood samples (600 μ l) were collected at 5, 10, 20, 30, 60 and 90 min after injection of labeled compound for determination of metabolites. Blood analysis was done by thin-layer chromatography (TLC). A plasma aliquot was developed on a silica gel TLC plate after drying. The eluant system was methanol:ethylacetate:triethylamine (10:90:0.01). At 5 min more than 90% of the activity was associated with ¹¹C-CFT, R_f = 0.45. The rest of the activity was associated with more polar metabolic product R_f = 0.1–0.2 (possibly hydrolysis of the 2B-carbomethoxy ester). The metabolic product increased >20% at 30 min. At later times low levels of radioactivity in blood did not allow for accurate quantification of the peaks.

Data Analysis. Imaging data were corrected for attenuation, decay and collection time. PET images were reconstructed using Hanning weighted convolution backprojection (28). Regions of interest (ROIs), including left and right caudate and putamen, frontal, parietal and temporal cortex, thalamus and cerebellum, were drawn on different planes and activity per unit volume, percent activity of injected dose and ligand concentration were calculated. The values corresponding to time points of 60 and 90 min were interpolated for each ROI. Putamen data were averages of data from A-P levels 20 and 15 mm from the left and right sides using the area of ROI as a weight. Caudate and cortical data were averaged similarly from A-P levels 25 and 20 mm from the left and right sides. Thalamus data were obtained from A-P level 10 mm and cerebellum data were averaged from levels –5 and –10 mm. In vivo specific binding for each subject was defined by the ratio of average radioactivity concentration in caudate, putamen, cortex and thalamus to the corresponding cerebellum value based on the assumption that the cerebellum does not have specific binding sites and the measured radioactivity represents nonspecific binding.

In studies involving MPTP-treated animals, the ROIs obtained during the pre-MPTP phase (control study) were used as guides, because the striatum is not clearly identifiable in brains of MPTP-treated monkeys.

RESULTS

Carbon-11-CFT PET Imaging

Time-activity curves were generated from various coronal images, which included planes of frontal cortex, caudate nu-

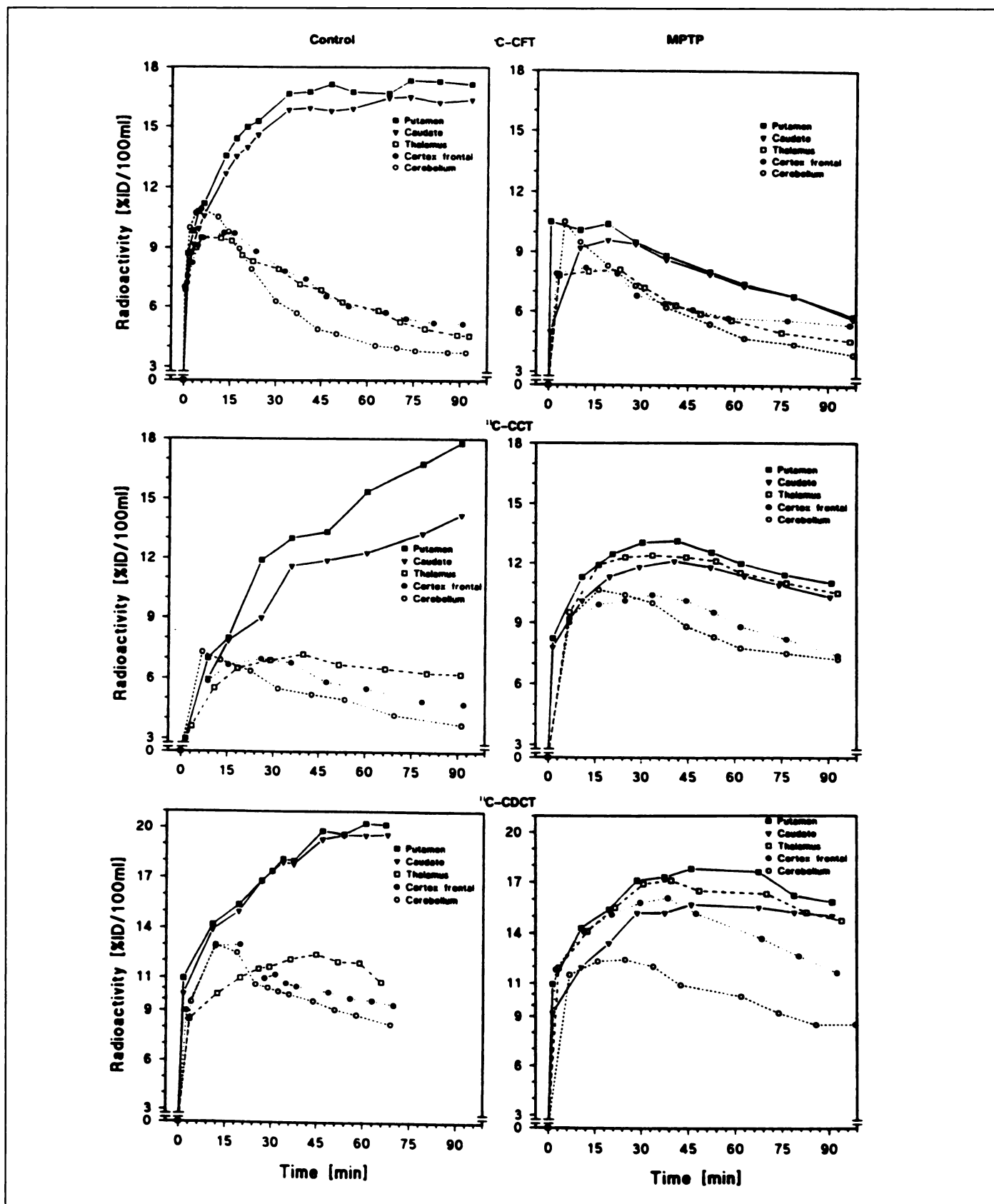


FIGURE 2. Time-activity distribution of ^{11}C -CFT, ^{11}C -CCT, and ^{11}C -CDCT in a control and MPTP-treated primate (*macaca fascicularis*) in five brain areas. Putamen data are the average of level 15 mm on the left and right sides, caudate data of level 20 mm, and frontal cortex data of level 25 mm, respectively. Thalamic data are obtained from level 10 mm and cerebellum data of level -5 mm.

cleus, putamen, thalamus and cerebellum. In Figure 2, putamen data are averaged from the left and right sides at A-P level 15 mm. Caudate data are averaged from the left and right sides at A-P level 20 mm. Data for frontal cortex are averaged from the

left and right sides at A-P level 25 mm. Thalamic data were obtained from A-P level 10 mm and cerebellar data were from level -5 mm. Time activity curves for ^{11}C -CFT in normal caudate and putamen showed a rapid increase in radioactivity

TABLE 1
Specific binding of [¹¹C]CFT, [¹¹C]CCT and [¹¹C]CDCT in Normal and MPTP-treated Primates at 60 and 90 Min*

PET imaging agent	Number of animals/studies	60 min				90 min			
		Caudate	Putamen	Frontal cortex	Thalamus	Caudate	Putamen	Frontal cortex	Thalamus
[¹¹ C]CFT	Control[5/5]	4.2 ± 0.8	4.9 ± 1.2	1.4 ± 0.2	1.4 ± 0.2	4.9 ± 1.2	5.5 ± 1.1	1.2 ± 0.2	1.1 ± 0.2
	MPTP [2/5]	1.4 ± 0.1	1.5 ± 0.1	1.2 ± 0.2	1.2 ± 0.2	1.3 ± 0.1	1.4 ± 0.3	1.2 ± 0.2	1.1 ± 0.1
[¹¹ C]CCT	Control[2/2]	2.7 ± 0.4	3.4 ± 0.3	1.2 ± 0.2	1.5 ± 0.3	3.7 ± 0.5	4.4 ± 0.6	1.3 ± 0.3	1.6 ± 0.3
	MPTP [1/1]	1.4 ± 0.4	1.5 ± 0.3	1.2 ± 0.2	1.5 ± 0.2	1.4 ± 0.4	1.6 ± 0.4	1.2 ± 0.2	1.5 ± 0.3
[¹¹ C]CDCT	Control[1/1]	2.3 ± 0.4	2.4 ± 0.5	1.2 ± 0.2	1.4 ± 0.2	—	—	—	—
	MPTP[1/1]	1.6 ± 0.4	1.8 ± 0.3	1.5 ± 0.2	1.8 ± 0.4	1.8 ± 0.2	1.9 ± 0.4	1.5 ± 0.2	1.8 ± 0.4

*Specific binding was determined as a ratio of uptake (mean ± s.d.) of each region [caudate = average from AP levels 25 and 20 mm on left and right sides; putamen = average from AP levels 20 and 15 mm on left and right sides; frontal cortex = average from AP levels 25 and 20 mm on left and right sides; thalamus from AP level 10 mm] to cerebellum (average from AP levels -5 and -10 mm).

over the first 10 min after injection and a slower increase up to 90 min (Fig. 2, top). In the cortex, thalamus and cerebellum radioactivity increased sharply within minutes but declined after 6–7 min. In MPTP-treated primates (Fig. 2, top right), radioactivity increased sharply in all brain regions although the plateau for putamen and caudate occurred later than for other regions. A rapid decline in all regions was observed.

For control studies interpolated values for specific binding ratios in caudate, putamen, frontal cortex and thalamus at 60 and 90 min are given in Table 1. The striatum-to-cerebellum ratio increased sharply to >4 within 60 min and was approximately 5 within 90 min. In the other brain areas, frontal cortex and thalamus, the ratios were equivalent and did not exceed 1.4 for the duration of the experiment. This distribution corresponds closely to known distribution of ³H-CFT (WIN 35,428) on the dopamine transporter, dopamine and dopamine receptors (19–23). In MPTP-treated primates, the striatum-to-cerebellum ratio was lightly higher at 60 min than at 90 min (1.4 and 1.5 versus 1.3 and 1.4) indicating washout of radioactivity. In addition, binding ratio in striatum was lightly higher than in cortex and thalamus, 1.2 at 60 min and 1.2 and 1.1 at 90 min, respectively. The distribution of ¹¹C-CFT in a normal and an MPTP-treated primate are compared at 4 different levels (20, 15, 10 and -5 mm) at 60–64 min after injection of the labeled ligand (Fig. 3).

Carbon-11-CCT PET Imaging

The regional accumulation of radioactivity following intravenous injection of monochloro analog of CFT, ¹¹C-CCT in normal and MPTP-treated monkeys was similar to that of ¹¹C-CFT (Fig. 2, middle panel). In the control caudate and putamen, the radioactivity increased through the imaging period (90 min) while the radioactivity washed out from other areas of brain. In MPTP-treated monkey brain radioactivity washed out of all brain areas. A relatively high striatum-to-cerebellum ratio was achieved (2.7 and 3.4) at 60 min, which increased to 3.7 and 4.4 by 90 min (Table 1). The thalamus-to-cerebellum ratio (1.5) was higher than the corresponding ratio for the frontal cortex.

Carbon-11-CDCT PET Imaging

In vitro, CDCT or dichloropropane, the dichloro analog of CFT has one of the highest affinities for the dopamine transporter (25). The time-activity curves for ¹¹C-CDCT revealed rapid accumulation in putamen and caudate, and significant levels in thalamus, frontal cortex and cerebellum in normal monkeys (Fig. 2, lower left panel). Radioactivity increased in caudate and putamen through the imaging period (70 min) and accumulated in the thalamus for at least 45 min while it decreased in frontal cortex and cerebellum after an initial rise. In an MPTP-treated animal, radioactivity increased and thereafter remained constant

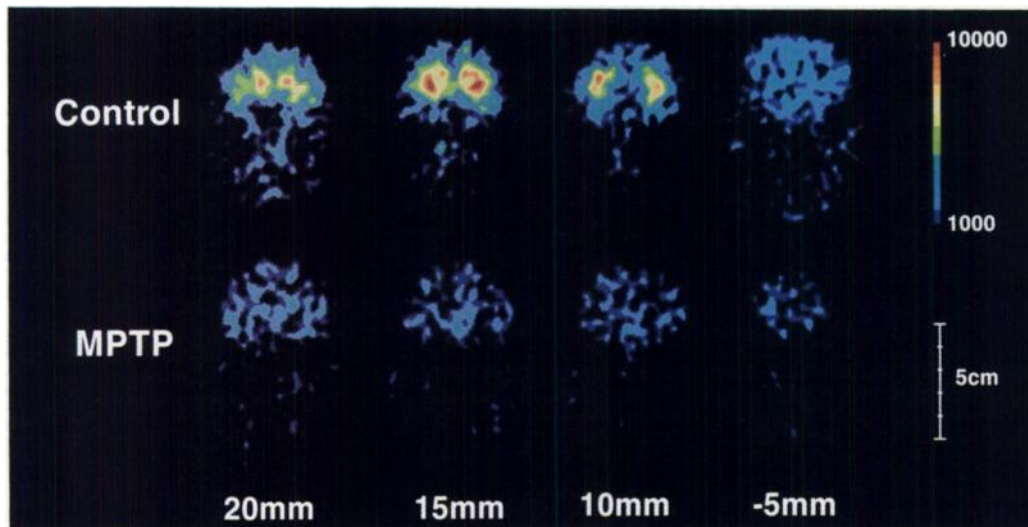


FIGURE 3. Distribution of ¹¹C-CFT at four coronal brain levels (20, 15, 10 and -5 mm) in a control (upper row) and MPTP-treated (lower row) primate at 60–64 min after injection. After corrections for decay, collection time and injected activity the highest pixel value of the eight images is normalized to 10,000 and the lowest to 0. All the images are normalized according to this scale.

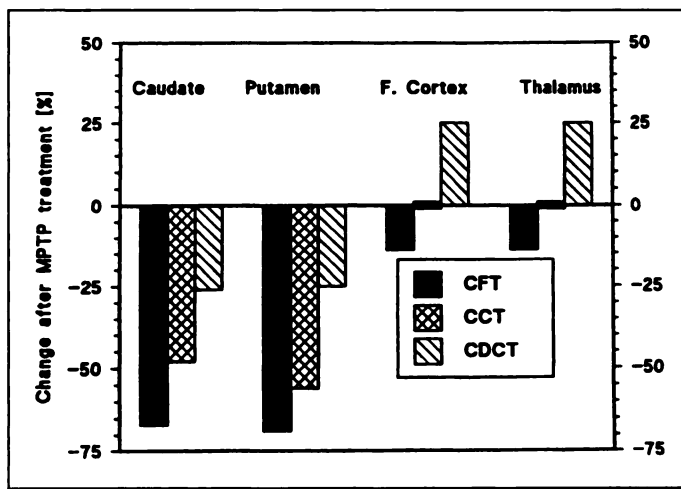


FIGURE 4. Average change in specific binding after MPTP treatment in four brain areas (putamen, caudate, frontal cortex and thalamus) using ^{11}C -CFT, ^{11}C -CCT and ^{11}C -CDCT at 60–64 min after injection of labeled ligand. Specific binding was defined as ratios of radioactivity concentrations to cerebellum basing on the assumption that cerebellar radioactivity represents nonspecific binding.

in the caudate, putamen and thalamus and declined in the cortex and cerebellum after an initial increase (Fig. 2, bottom right panel). In a control study the binding ratios were 2.3 and 2.4 for caudate and putamen and 1.2 and 1.4 for cortex and thalamus at 60 min (Table 1). In an MPTP-treated monkey the thalamus/cerebellum ratio (1.8) was the same as the putamen/cerebellum ratio at 60 min. However, at 90 min the binding ratio of putamen (1.9) was lightly higher than that of thalamus. The thalamus to cerebellum ratio was higher than frontal cortex to cerebellum ratio in both the control and MPTP-treated primate brain.

Comparison of Carbon-11-CFT, CCT and CDCT in MPTP-Treated Monkeys

The loss of specific binding in striatum after MPTP treatment differed for ^{11}C -CFT, ^{11}C -CCT and ^{11}C -CDCT (Table 1, Fig.

4). The largest loss was detected using CFT, indicating that ^{11}C -CFT is the most sensitive of the three ligands for detecting loss of dopamine transporters. In a comparative distribution of the three ligands in MPTP-treated primates at levels 20, 15, 10 and -5 mm binding can clearly be seen in extrastriatal regions (e.g., thalamus) for the chlorinated ligands (Fig. 5).

DISCUSSION

The development of selective high-affinity ligands for imaging the dopamine transporter on dopamine neurons is desirable for a number of reasons. The higher the affinity of the drug, the lower the dose needed for detecting its targets by in vivo imaging, and the more likely the ligand will remain associated with its target for the duration of the study. Furthermore, dopamine may compete with the probe for binding to the dopamine transporter if the affinity is low. Finally, selectivity is needed to minimize binding to the serotonin transporter or other sites, as nonspecific binding may reduce the level of accuracy of imaging data.

The affinity and selectivity of ^{11}C -CFT, ^{11}C -CCT and ^{11}C -CDCT were previously determined in vitro (24). The IC_{50} -values for the dopamine transporter were 11.0 ± 1.0 nM for CFT, 1.40 ± 0.04 nM for CCT (RTI-131) and 1.09 ± 0.02 nM for CDCT. Corresponding values for the serotonin transporter were 160 ± 20 nM, 5.87 ± 2.8 nM and 2.47 ± 0.14 nM. Transporter selectivities (dopamine/serotonin) calculated from the in vitro data were 15-fold for CFT, 4-fold for CCT and 2-fold for CDCT. Thus, CFT is the most selective of the three phenyltropane analogs, although it has lower affinity than the other halogenated phenyltropane analogs. The imaging data supports these observations. The specific binding expressed as striatum/cerebellum ratio was highest using ^{11}C -CFT; 4.9 ± 1.2 at 60 min and 5.5 ± 1.1 at 90 min for putamen and lowest with ^{11}C -CDCT, 2.4 ± 0.5 in putamen at 60 min. Further, the loss in specific binding after MPTP treatment was most prominent when ^{11}C -CFT was used to image the striatum (Figs. 4, 5). Interestingly, using ^{11}C -CDCT, the calculated specific binding ratio in cortex area and thalamus increased after MPTP treat-

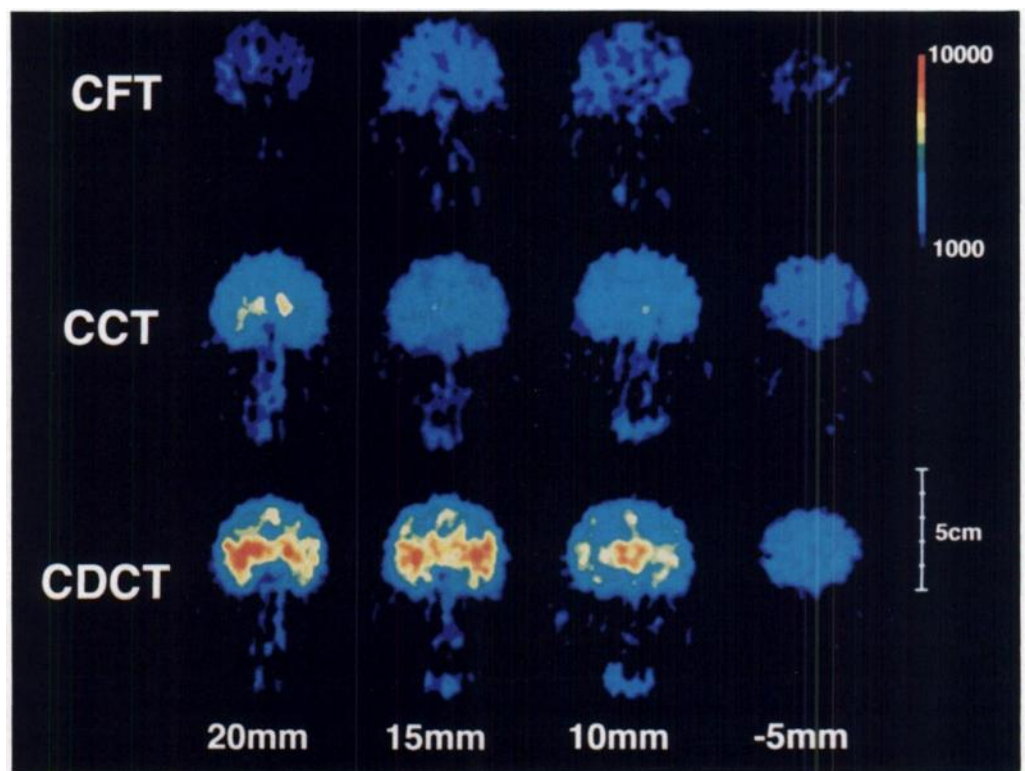


FIGURE 5. Comparative distribution of the ligands ^{11}C -CFT, ^{11}C -CCT and ^{11}C -CDCT in MPTP-treated primates at four coronal brain levels (20, 15, 10 and -5 mm) at 60–64 min after injection. The normalization of image set is the same as in Figure 3.

ment in a single study. These areas contain moderately high level of the serotonin transporter and as ^{11}C -CDCT has high affinity (2.47 nM) for serotonin transporters, it may bind to these sites when the dopamine transporter is depleted after MPTP treatment. Taken together, the studies support the use of more selective agents for monitoring dopamine terminals in neurodegenerative diseases.

It is shown that tracer/receptor complex may be affected by radioactive metabolites and changes in blood flow (29). However, metabolism of CFT is minimal (23) and the observed metabolite structure is different than that of the ^{11}C -CFT. The main metabolite is a less lipophilic compound, the hydrolyzed methylester and its affinity is one order of magnitude lower than the labeled parent compound. This strongly suggests that ^{11}C -labeled metabolites do not significantly affect PET imaging studies. In addition, ketamine anesthesia may decrease blood flow thereby affecting the absolute values obtained. However, in this study specific binding was determined by measuring the ratio of uptake to cerebellar accumulation of radioactivity, thereby minimizing errors that may be related to blood flow.

The specific binding ratios of ^{11}C -CFT (4.2 ± 0.8 for caudate and 4.9 ± 1.2 for putamen at 60 min and 4.9 ± 1.2 and 5.5 ± 1.1 at 90 min) in primates are similar to the corresponding ratios in humans, published by Wong et al. (30). However, the striatal-cerebellar ratios for the baboon reported by the group, were significantly lower. This may be explained by partial volume effect, since the resolution of the imaging devices used in their studies was 6 or 8 mm and data were not corrected for recovery. Optimally, the resolution of the imaging device should be at least half of the size of the object imaged to avoid partial volume effects (31). The PET tomograph used in the present study with a FWHM resolution of 4.5 mm, is one-half the size of the cynomolgus caudate-putamen complex (32), greatly reduces partial volume effects.

Recently, another potent halogenated phenyltropane analog first proposed in 1990 (20), was introduced. β -CIT or RTI-55 (2B-carbomethoxy-3B-(4-iodophenyl)tropane) has been tested both in PET and SPECT (33–36). This compound has a high specific binding ratio in striatum (5.6) and a high binding ratio for midbrain (2.2). However, this compound accumulates in lungs (23), a potential depot for drugs that are potent inhibitors of serotonin transport (22) and in brain regions other than striatum. It requires 4 hr for the ligand to clear from these regions before a difference of 30–40% between normal and Parkinson's diseased brains become apparent and 22 hr to detect a 60–70% difference (29).

CFT was the first ligand in the phenyltropane series to demonstrate a loss of dopamine neurons equivalent to the loss of dopamine in the human postmortem Parkinson's diseased brain (21). Subsequently, ^{11}C -CFT binding was found to correlate with behavioral symptoms in a primate model of Parkinson's disease (37,38) and in early Parkinson's disease in humans (30,39). The present results clearly indicate that ^{11}C -CFT has the highest selectivity of the three ligands studied and despite its moderate affinity, is a very promising ligand for monitoring dopamine neuron degeneration. Carbon-11-CFT may be useful for detecting Parkinson's disease in the presymptomatic phase and enable introduction of drugs that retard disease progression as suggested previously by Kaufman and Madras (21).

ACKNOWLEDGMENTS

We thank MaryAnn Crowley for her excellent technical assistance during the PET studies; cyclotron operators William Bucklewicz and Larry Beagle for their contributions; Cao-Huu Tuan,

PhD, John Zaknun, MD, Department of Radiology, and Steven B. Tatter, MD, Department of Neurosurgery, Massachusetts General Hospital for helping with the image production. This work was supported in part by National Institutes of Health grant CA32873-11 and Department of Energy grant DE-FG02-87ER60519 to Massachusetts General Hospital and grants DA06303, NS30556, RR00168 and National Institute on Drug Abuse Grant DA09462 to the Primate Center. A preliminary report of this work appeared in the 1994 proceedings of the annual meeting of the Society Nuclear Medicine.

REFERENCES

- Bernheimer H, Birkmayer W, Hornykiewicz O. Brain dopamine and the syndromes of Parkinson and Huntington. Clinical, morphological and neurochemical correlations. *J Neurol Sci* 1973;20:415–455.
- Kish SJ, Shannak K, Hornykiewicz O. Uneven pattern of dopamine loss in the striatum of patients with idiopathic Parkinson's disease. Pathophysiologic and clinical implications. *N Engl J Med* 1988;318:876–878.
- Poirier LT, Sourkes TL. Influence of the substantia nigra on the catecholamine content of striatum. *Brain* 1969;88:181–189.
- Davis GC, Williams AC, Markey SP, et al. Chronic parkinsonism secondary to intravenous injection of meperidine analogues. *Psychiatry Res* 1979;1:249–254.
- Langston JW, Forno LS, Rebert CS, Irwin I. Selective nigral toxicity after systemic administration of 1-methyl-4-phenyl-1,2,3,6-tetrahydropyridine (MPTP) in the squirrel monkey. *Brain Res* 1984;292:390–394.
- Burns RS, Chiueh CC, Markey SP, et al. A primate model of Parkinsonism: selective destruction of dopaminergic neurons in the pars compacta of the substantia nigra by N-methyl-4-phenyl-1,2,3,6-tetrahydropyridine. *Proc Natl Acad Sci USA* 1983;80:4546–4550.
- Smith RD, Zhang Z, Kurlan R, et al. Developing a stable bilateral model of parkinsonism in rhesus monkeys. *Neuroscience* 1993;52:7–16.
- Calne DDB, Langston JW, Martin WRW, et al. Positron emission tomography after MPTP: observations relating to the cause of Parkinson's disease. *Nature* 1985;317:244–248.
- Sawle GV, Playford ED, Burn DJ, et al. Separating Parkinson's disease from normality: discriminant function analysis of fluorodopa F-18 positron emission tomography data. *Arch Neurol* 1994;51:237–243.
- Lindvall O, Sawle G, Widner H, et al. Evidence for long-term survival and function of dopaminergic grafts in progressive Parkinson's disease. *Ann Neurol* 1994;35:172–180.
- Aquilonius S-M, Bergstrom K, Eckernas S-A, et al. In vivo evaluation of striatal dopamine reuptake sites using ^{11}C -nomifensine and positron emission tomography. *Acta Neurol Scand* 1987;76:283–287.
- Salmon E, Brooks DJ, Leenders KL, et al. A two-compartmental description and kinetic procedure for measuring regional cerebral [^{11}C]nomifensine uptake using positron emission tomography. *J Cereb Blood Flow Metab* 1990;10:307–316.
- Kilbourn MR. In vivo binding of [^{18}F]GRB 13119 to the brain dopamine uptake system. *Life Sci* 1988;42:1347–1353.
- Ciliax BJ, Kilbourn MR, Haka MS, Penney JB. Imaging the dopamine uptake site ex vivo [^{18}F]GRB 13119 binding autoradiography in rat brain. *J Neurochem* 1990;55:619–623.
- Kilbourn MR, Sherman PS, Pisani T. Repeated reserpine administration reduces in vivo [^{18}F]GRB 13119 binding to the dopamine uptake site. *Eur J Pharmacol* 1992;216:109–112.
- Fowler JS, Volkow ND, Wolf AP, et al. Mapping cocaine binding sites in human and baboon brain in vivo. *Synapse* 1989;4:371–377.
- Gatley SJ, Yu D-W, Fowler JS, et al. Studies with differentially labeled [^{11}C]cocaine, [^{11}C]norcocaine, [^{11}C]benzoylcegonine and [^{11}C] and 4'-[^{18}F]fluorococaine to probe the extent to which [^{11}C]cocaine metabolites contribute to PET images of the baboon brain. *J Neurochem* 1994;62:1154–1162.
- Madras BK, Spealman RD, Fahey MA, et al. Cocaine receptors labeled by [^3H]2B-carbomethoxy-3B-(4-fluorophenyl)tropane. *Mol Pharmacol* 1989;36:518–524.
- Madras BK. ^{11}C -WIN 35,428 for detecting dopamine depletion in mild Parkinson's disease. *Ann Neurol* 1994;35:376–377.
- Canfield DR, Kaufman MJ, Madras BK. Autoradiographic localization of cocaine receptors by [^3H] CFT in monkey brain. *Synapse* 1990;5:189–195.
- Kaufman MJ, Madras BK. Severe depletion of cocaine recognition sites associated with the dopamine transporter in Parkinson's diseased striatum. *Synapse* 1991;9:43–49.
- Kaufman MJ, Madras BK. Cocaine recognition sites labeled by [^3H]CFT and [^{125}I]RTI-55 in monkey brain. II. Ex vivo autoradiographic distribution. *Synapse* 1992;12:99–111.
- Madras BK, Elmaleh DR, Meltzer PC, et al. Positron emission tomography of cocaine binding sites on the dopamine transporter. In: Sorer H, Rapaska RS, eds. *Imaging techniques in medications development: preclinical and clinical aspects*. Rockville, MD: National Institute on Drug Abuse; NIDA Research Monograph 1994;138:57–69.
- Meltzer PC, Liang AY, Brownell A-L, et al. Substituted 3-phenyltropane analogs of cocaine: synthesis, inhibition of binding at cocaine recognition sites, and positron emission tomography imaging. *J Med Chem* 1993;36:855–862.
- Carroll FI, Lewin AH, Abraham P, et al. Synthesis and ligand binding of cocaine isomers at the cocaine receptor. *J Med Chem* 1991;34:883–886.
- Carroll FI, Lewin AH, Boja JW, Kuhar MJ. Cocaine receptor: biochemical characterization and structure activity relationships of cocaine analogues at the dopamine transporter. *J Med Chem* 1992;35:969–981.
- Brownell GL, Burnham CA, Chesler DA. High-resolution tomograph using analog

- coding. In: Greitz T, Ingvar DH, Widen L, eds. *The metabolism of the human brain studied with positron emission tomography*. New York, NY: Raven Press; 1985:13-19.
28. Chesler DA. Positron tomography and three-dimensional reconstruction technique. In: Freedman GS, ed. *Tomographic imaging in nuclear medicine*. New York, NY: Society of Nuclear Medicine; 1973:374-378.
 29. Laruelle M, Wallace E, Seibyl JP, et al. Graphical, kinetic and equilibrium analyses of in vivo [¹²³I]β-CIT binding to dopamine transporters in healthy human subjects. *J Cereb Blood Flow Metab* 1994;14:982-994.
 30. Wong DF, Yung B, Dannals RF, et al. In vivo imaging of baboon and human dopamine transporters by positron emission tomography using [¹¹C]WIN 35,428. *Synapse* 1993;15:130-142.
 31. Hoffman EJ, Huang S-C, Phelps ME. Quantitation in positron emission computed tomography. I. Effect of object size. *J Comp Assist Tomogr* 1979;3:299-308.
 32. Szabo J, Cowan WM. A stereotactic atlas of the brain of the cynomolgus monkey (*macaca fascicularis*). *J Comp Neurol* 1984;222:265-300.
 33. Carroll FI, Rahman MA, Abraham P, et al. Iodine-123-3β-(4-iodophenyl)tropan-2β-carboxylic acid methyl ester (RTI-55), a unique cocaine receptor ligand for imaging the dopamine and serotonin transporters in vivo. *Med Chem Res* 1991;1:289-294.
 34. Neumeyer JL, Wang S, Milius RA, et al. [¹²³I]2β-carbomethoxy-3β-(4-iodophenyl)tropane (β-CIT): high affinity SPECT radiotracer of monoamine reuptake sites in brain. *J Med Chem* 1991;34:144-146.
 35. Boja JM, Mitchell WM, Patel A, et al. High-affinity binding of [¹²⁵I]RTI-55 to dopamine and serotonin transporters in rat brain. *Synapse* 1992;12:27-36.
 36. Muller L, Halldin C, Farde L, et al. [¹¹C]β-CIT, a cocaine analogue. Preparation, autoradiography and preliminary PET investigations. *Nucl Med Biol* 1993;20:249-255.
 37. Hantraye P, Brownell A-L, Elmaleh D, et al. Dopamine fiber detection by [¹¹C]-CFT and PET in a primate model of Parkinsonism. *Neuro Report* 1992;3:265-268.
 38. Wullner U, Pakzaban P, Brownell A-L, et al. Dopamine terminal loss and onset of motor symptoms in MPTP-treated monkeys: a positron emission tomography study with [¹¹C]-CFT. *Exp Neurol* 1994;126:305-309.
 39. Frost JJ, Rosier AJ, Reich SG, et al. Positron emission tomographic imaging of the dopamine transporter with [¹¹C]-WIN 35,428 reveals marked declines in mild Parkinson's disease. *Ann Neurol* 1993;34:423-431.

Age-Related Diminution of Dopamine Antagonist-Stimulated Vesamicol Receptor Binding

Simon M.N. Efange, Rosemary B. Langason and Anil B. Khare

Departments of Radiology, Medicinal Chemistry and Neurosurgery, University of Minnesota, Minneapolis, Minnesota

Previous studies of radiolabeled vesamicol receptor (VR) ligands suggest that the latter may be used in conjunction with dopamine D2 antagonists to measure changes in striatal cholinergic function. In this study, the effects of aging on vesicular acetylcholine storage/release were investigated with the high-affinity VR ligand (+)-meta-[¹²⁵I]iodobenzyltrozamicol [(+)-[¹²⁵I]MIBT]. **Methods:** Male Fischer 344 rats (aged 3 and 24 mo) were injected either with a vehicle or a D2 antagonist [haloperidol or S(-)-eticlopride]. At prescribed intervals thereafter, all animals were intravenously injected with 10 μCi of (+)-[¹²⁵I]MIBT. Three hours after radiotracer injection, the animals were killed and their brains dissected. The concentration of radiotracer in the striatum, cortex and cerebellum were then determined. **Results:** In control animals, comparable levels of (+)-[¹²⁵I]MIBT were observed in corresponding brain regions of young adult and aged Fischer 344 rats. Moreover, in haloperidol- and S(-)-eticlopride-treated young adult rats, striatal levels of (+)-[¹²⁵I]MIBT were elevated by 35% and 66%, respectively, relative to controls. In contrast, haloperidol treatment failed to alter the striatal levels of (+)-[¹²⁵I]MIBT in aged rats while S(-)-eticlopride displayed a two-fold reduction in potency in aged rats. **Conclusion:** Aging is associated with a reduction in striatal cholinergic plasticity or *striatal cholinergic reserve* and that the D2-stimulated increase in VR ligand binding is a functionally relevant parameter.

Key Words: iodine-125-MIBT vesamicol receptor; cholinergic function; aging

J Nucl Med 1996; 37:1192-1197

The cholinergic system has been implicated in memory and central motor functions (1-3). In age-related neurologic disorders, such as Alzheimer's disease, a progressive neurodegenerative disorder associated with: loss of cognitive function and changes in personality, marked reductions in the presynaptic cholinergic markers choline acetyltransferase (ChAT), acetyl cholinesterase (AChE) and sodium dependent high-affinity choline transport (SDHACHT) have been observed in several

specific regions of the brain (4-7). Although qualitatively similar alterations in cognitive and motor function are associated with normal aging and age-related neuropathology, investigations into the neurochemistry of normal aging have largely yielded conflicting results.

With normal aging, alterations in presynaptic cholinergic markers are either absent or of a much lower magnitude than in age-related neuropathology (3,8,9). In spite of these growing body of evidence suggests that the dynamic aspects of central cholinergic neurotransmission are impaired in aging (10). Specifically, studies of SDHACHT (an indicator of ongoing neuronal activity and structural integrity) and vesicular acetylcholine ACh (1) release in rodents have consistently revealed significant age-related reductions (10-13). In the present study, we attempt to assess the effects of aging on ACh storage/release mechanisms with the aid of the radiolabeled vesamicol receptor (VR) ligand (+)-meta-[¹²⁵I]iodobenzyltrozamicol ((+)-[¹²⁵I]MIBT) (14).

The vesamicol receptor, a unique site on the cholinergic synaptic vesicle, is functionally linked to the vesicular acetylcholine (ACh) transporter (15). The prototypical ligand for the VR, (-)-2-(4-phenylpiperidinyl)cyclohexanol (AH5183, vesamicol; Fig. 1), is a potent noncompetitive inhibitor of ACh storage (16). Binding of vesamicol to the VR results in the blockade of cholinergic neurotransmission, attributable to the inhibition of both vesicular ACh storage and the subsequent quantal release of ACh. ACh synthesis is, however, unaffected. The location of this receptor presents opportunities for studying the mechanisms underlying the storage and release of ACh. As part of our ongoing effort to validate the use of radiolabeled VR ligands in the study of presynaptic cholinergic function, we demonstrate in this article, with the aid of the VR ligand (+)-[¹²⁵I]MIBT, that aging is accompanied by a diminution of striatal cholinergic function.

MATERIALS AND METHODS

The radiotracers (+)- and (-)-[¹²⁵I]MIBT were synthesized as described (14) at a specific activity of 1500 ± 200 Ci/mmol.

Received Jun. 2, 1995; revision accepted Oct. 18, 1995.

For correspondence or reprints contact: S.M.N. Efange, PhD, University of Minnesota Hospital and Clinic, Department of Radiology, Mayo Box 292, 420 Delaware St. S.E., Minneapolis, MN 55455.